HHS Public Access

Author manuscript

Am J Surg Pathol. Author manuscript; available in PMC 2019 May 22.

Published in final edited form as:

Am J Surg Pathol. 2018 January ; 42(1): 18–27. doi:10.1097/PAS.0000000000000933.

Epithelial-Myoepithelial Carcinoma:

Frequent Morphologic and Molecular Evidence of Preexisting Pleomorphic Adenoma, Common HRAS Mutations in PLAG1-intact and HMGA2-intact Cases, and Occasional TP53, FBXW7, and SMARCB1 Alterations in High-grade Cases

Soufiane El Hallani, MD, PhD[*], **Aaron M. Udager, MD, PhD**[†], **Diana Bell, MD**[‡], **Isabel Fonseca, MD**[§], **Lester D.R. Thompson, MD**[‖], **Adel Assaad, MD**[¶], **Abbas Agaimy, MD**[#], **Alyssa M. Luvison, BS**[*], **Caitlyn Miller, BS**[*], **Raja R. Seethala, MD**[*], and **Simion Chiosea, MD**[*]

[*]Department of Pathology, University of Pittsburgh Medical Center, Pittsburgh, PA;

[†]Department of Pathology, Michigan Medicine, Ann Arbor, MI;

[‡]Department of Pathology, The University of Texas MD Anderson Cancer Center, Houston, TX;

[§]Pathological Anatomy Institute, Faculdade de Medicina, Universidade de Lisboa & Serviço de Anatomia Patológica, Instituto Português de Oncologia Francisco Gentil, Lisboa, Portugal;

[‖]Department of Pathology,Southern California Permanente Medical Group, Woodland Hills, CA;

[¶]Department of Pathology, Virginia Mason Hospital, Seattle, WA;

[#]Institute of Pathology, University Hospital, Erlangen, Germany.

Abstract

We hypothesized that there is a relationship between the preexisting pleomorphic adenoma [PA]), histologic grade of epithelial-myoepithelial carcinomas (EMCAs), and genetic alterations. EMCAs (n = 39) were analyzed for morphologic and molecular evidence of preexisting PA (*PLAG1, HMGA2* status by fluorescence in situ hybridization, FISH, and *FGFR1-PLAG1* fusion by next-generation sequencing, NGS). Twenty-three EMCAs were further analyzed by NGS for mutations and copy number variation in 50 cancer-related genes. On the basis of combined morphologic and molecular evidence of PA, the following subsets of EMCA emerged: (a) EMCAs with morphologic evidence of preexisting PA, but intact *PLAG1* and HMGA2 (12/39, 31%), (b) Carcinomas with *PLAG1* alterations (9/39, 23%), or (c) *HMGA2* alterations (10/39, 26%), and (d) de novo carcinomas, without morphologic or molecular evidence of PA (8/39, 21%). Twelve high-grade EMCAs (12/39, 31%) occurred across all subsets. The median disease-free survival was 80 months (95% confidence interval, 77–84 mo). Disease-free survival and other clinicopathologic parameters did not differ by the above defined subsets. HRAS mutations were more common in EMCAs with intact *PLAG1* and *HMGA2* (7/9 vs. 1/14, P < 0.001). Other genetic abnormalities (TP53 [n = 2], *FBXW7* [n = 1], *SMARCB1* deletion [n = 1]) were seen only in high-grade EMCAs with intact *PLAG1* and *HMGA2*. We conclude that most EMCAs arose ex PA (31/39,

Correspondence: Simion Chiosea, MD, UPMC, Presbyterian University Hospital, A610-2, 200 Lothrop St, Pittsburgh, PA 15213 (chioseasi@upmc.edu).

Conflicts of Interest and Source of Funding: The authors have disclosed that they have no significant relationships with, or financial interest in, any commercial companies pertaining to this article.

80%) and the genetic profile of EMCA varies with the absence or presence of preexisting PA and its cytogenetic signature. Progression to higher grade EMCA with intact *PLAG1* and *HMGA2* correlates with the presence of TP53, *FBXW7* mutations, or *SMARCB1* deletion.

Keywords

epithelial-myoepithelial carcinoma; carcinoma ex pleomorphic adenoma; *PLAG1*; *HMGA2*

Epithelial-myoepithelial carcinoma (EMCA) is a salivary tumor with dual cell population: luminal ductal cells and outer myoepithelial cells, classically with clear cytoplasm.[1–4] EMCA was initially described by Donath et al[4] and was previously referred to as adenomyoepithelioma, clear cell adenoma, or carcinoma. Although rare cases of high-grade EMCA have been reported,[3,5–8] most commonly, EMCAs are low-grade tumors and have to be distinguished from pleomorphic adenoma (PA). Infiltrative growth, sharp demarcation from hypocellular hyalinized stroma, retraction (split) artifact between the ductal and abluminal myoepithelial cells are characteristic of EMCA. Such histologic findings form distinct areas when EMCA arises in a PA and help to distinguish EMCA from a merely cellular PA. Although, in practice, EMCA often has to be distinguished from PA, the prevalence of preexisting PA in EMCA is unknown.

PA was the first benign human epithelial neoplasm to be shown to harbor recurrent cytogenetic abnormalities, that is, rearrangements involving *Pleomorphic Adenoma Gene 1* (*PLAG1*) and *High Mobility Group A2* (*HMGA2*).[9,10] It has been recognized that there are several cytogenetically defined groups of PA, including those with *PLAG1* or *HMGA2* rearrangements (in up to 40%). *PLAG1* and *HMGA2* status, therefore, may complement morphology in identifying carcinomas ex PA.[11–13]

The genetic events leading to an EMCA likely depend on the precursor lesion (ie, PA or intercalated duct hyperplasia[14]) and may involve alterations of *TP53* and Harvey rat sarcoma viral oncogene homolog (HRAS). Up to 33% of EMCAs may harbor HRAS codon 61 mutations.[15,16]

Here, we aimed to determine the prevalence of preexisting PA in a series of EMCAs, characterize the frequency of *PLAG1* and *HMGA2* abnormalities, correlate *PLAG1* and *HMGA2* status with clinicopathologic features, and, finally, to characterize the relationship between the presence of preexisting PA and mutations and copy number variations in 50 cancer-related genes.

MATERIALS AND METHODS

Patients and Histologic Review

This study was approved by the Institutional Review Board (IRB991206). Tumors were categorized as follows: conventional (low grade by definition) EMCA, oncocytic, and apocrine variants,[3,17] EMCA ex PA, and high-grade EMCA. Conventional EMCAs were characterized by dual cell population with about 1:1 ratio of outer myoepithelial cells to inner luminal ductal cells. High-grade EMCA was defined by areas with the predominance

(overgrowth) of either myoepithelial or epithelial components with necrosis and nuclear pleomorphism.[5,6] Chondroid or myxoid stroma with benign ductal elements and hyalinized (to variable extent) hypocellular nodules were both accepted as morphologic evidence for preexisting PA. Clinicopathologic features of 13 cases were previously reported by Fonseca et al[2] and 6 cases were included in prior studies by our group.[3,8,16,17] Tumors were staged according to the 7th edition of the American Joint Committee on Cancer.[18]

Immunohistochemistry

Immunohistochemical staining for SMARCB1/INI-1 was performed with antibody from BD Transduction Laboratories, clone 25/BAF47, San Jose, CA.

Fluorescence In Situ Hybridization

PLAG1 and *HMGA2* rearrangements were detected by break-apart fluorescence in situ hybridization (FISH) probes (Empire Genomics, Buffalo, NY). Hyperploidy or amplification (centromeric enumeration probes were not used) was defined as presence of >2 signals in >75% of cells. To detect copy number alterations of the *SMARCB1* (*INI-1*) gene locus, FISH was performed using the ZytoLight SPEC SMARCB1/22q12 Dual Color Probe, which is a mixture of a green fl 22q12 Dua direct labeled SPEC *SMARCB1* probe hybridizing to the human *SMARCB1* gene in the chromosomal region 22q11.23 and an orange fluorochrome direct labeled SPEC 22q12 probe as supplied by the manufacturer (Zyto-Vision GmbH, Bremerhaven, Germany). Fifty to 100 cells per case were analyzed using Leica Biosystems FISH Imaging System (CytoVision FISH Capture and Analysis Workstation, Buffalo Grove, IL). Only cases with technically successful *PLAG1* and *HMGA2* FISH were included in this study.

Library Preparation, Sequencing, and Data Analysis

DNA extraction and targeted next-generation sequencing analysis were performed as described previously.[13] Library concentration and amplicon sizes were determined using TapeStation System (Agilent Technologies, Santa Clara, CA). Subsequently, the multiplexed barcoded libraries were enriched by clonal amplification using emulsion PCR on templated Ion Sphere Particles and loaded on Ion 318 Chip. Massively parallel sequencing was carried out on an Ion Torrent Personal Genome Machine sequencer (Life Technologies, Carlsbad, CA) using the Ion Personal Genome Machine Sequencing 200 Kit version 2 according to the manufacturer's instructions. After a successful sequencing reaction, the raw signal data were analyzed using Ion Torrent platform-optimized Torrent Suite version 4.0.2 (Life Technologies). The short sequence reads were aligned to the human genome reference sequence (GRCh37/hg19). Variant calling was performed using Variant Caller version 4.0 plugin (integrated with Torrent Suite) that generated a list of detected sequence variations in a variant calling file (VCF version 4.1; http://www.1000genomes.org/wiki/analysis/ variant %20call%20format/vcf-variant-call-format-version-41). The variant calls were annotated, filtered and priori-tized using SeqReporter,[19] an in-house knowledgebase and the following publically available databases; COSMIC v68 (http://cancer.sanger.ac.uk/cancergenome/projects/cosmic/), dbSNP build 137 (http://www.ncbi.nlm.nih.gov/SNP/), in silico prediction scores (PolyPhen-2 and SIFT) from dbNSFP light version 1.3.[20] Sequence variants with at least 300× depth of coverage and mutant allele frequency of > 5% of the total reads were

included for analysis. Copy number variations and gene fusions were identified by NGS as described previously.[21,22]

Statistical Analyses

Demographic and clinical comparison among subsets of EMCA was conducted with the Wilcoxon test for continuous data and the Fisher exact test or a χ^2 test for discrete data. Disease-free survival (DFS) was analyzed with a log rank test. A *P*-value of <0.05 was considered significant.

RESULTS

The clinicopathologic parameters of 39 patients with EMCA are summarized in Tables 1 and 2. Two thirds of patients were female and most patients presented with clinical stage I or II disease involving major salivary glands. Twenty-seven of 39 (69%) EMCAs were conventional, including oncocytic (n=1) and apocrine (n=1) variants (see Seethala et al[17] for detailed description). Of 12 high-grade EMCAs, 11 showed overgrowth and coagulative necrosis of myoepithelial component, while 1 case was characterized by overgrowth and comedo-type necrosis of the ductal component (Fig. 1). All high-grade EMCAs had conventional component. Morphologically, 30 of 39 (77%) EMCAs showed preexisting PA. In 4 cases, only recurrence with carcinoma was available for review and the initial resections, while diagnosed as PA, were not available for rereview for this study. The preexisting PA was represented by chondromyxoid stroma (n=9, including 3 cases with squamous metaplasia), hyalinized stroma (n=9), hyalinizing chondroid stroma (n=3), myxoid and hyalinizing stroma (n =2), myxoid stroma (n=2), and chondroid stroma with osseous and squamous metaplasia (n=1) (Figs. 2, 3).

Adequate follow-up was available for 25 patients. None of the clinicopathologic parameters (eg, sex, age, tumor site, grade, stage) differed by origin of EMCA (de novo vs. ex PA, as defined by morphology) and was not associated with DFS. The estimated median DFS for patients with EMCA was 80 months (95% confidence interval, 77–84 mo). Four patients developed recurrences 5 years after the initial surgery. Since this cohort included a significant number of high-grade EMCAs, DFS of patients with EMCA was compared with DFS of patients with salivary duct carcinoma (SDC), another carcinoma commonly arising in PA.[13] DFS for patients with EMCA was longer than DFS for patients with SDC, 37 months (95% confidence interval, 28–46 mo) (Fig. 4).

Subsets of EMCA Defined by Morphologic Evidence of PA and Status of *PLAG1* and *HMGA2*

Of 39 cases of EMCA, 10 cases were *HMGA2* positive (10/39, 26%), including 4 cases with rearrangement only (Fig. 3), 3 cases with rearrangement and hyperploidy (Fig. 5), and 3 cases with hyperploidy only. Of cases with *HMGA2* rearrangement, the median proportion of cells with rearrangement was 73% (range, 28% to 93%).

Nine cases of EMCA were *PLAG1* positive (9/39, 23%), including 4 cases with rearrangement only and 3 cases with rearrangement and hyperploidy as identified by FISH (Fig. 6). Of cases with *PLAG1* rearrangement, the median proportion of cells with

rearrangement was 90% (range, 75% to 98%). All EMCAs with *HMGA2* and *PLAG1* intact by FISH were tested by next-generation sequencing (NGS) for the intrachromosomal Fibroblast Growth Factor Receptor 1 (*FGFR1*)-*PLAG1* fusion and 2 cases with *FGFR1*-*PLAG1* fusion were identified.

On the basis of the morphologic evidence of PA and *HMGA2* and *PLAG1* status, EMCA can be categorized into several subsets (Fig. 7). Overall, 80% (31/39) of EMCA originated from PA. Patients' DFS, sex, age, histologic grade, tumor site, pT, pN, and clinical stage did not correlate with these subsets of EMCA.

Relationship Between the Subsets of EMCA and Genetic Alterations in 50 Cancer-related Genes

Twenty-three cases had sufficient material for NGS testing. The relationship between the EMCA's subsets and histologic grade, mutations and/or copy number variation of *SMARCB1*, *FBXW7*, TP53, PIK3CA, and HRAS is shown in Figure 8.

The genes listed below were negative for mutations and copy number alterations: ABL1, *AKT1*, *ALK*, *APC*, *ATM*, *BRAF*, *CDH1*, *CDKN2A*, *CSF1R*, *CTNNB1*, *EGFR*, *ERBB2*, *ERBB4*, *EZH2*, *FGFR1*, *FGFR2*, *FGFR3*, *FLT3*, *GNA11*, *GNAS*, *GNAQ*, *HNF1A*, *IDH1*, *IDH2*, *JAK2*, *JAK3*, *KDR*, *KIT*, *KRAS*, *MET*, *MLH1*, *MPL*, *NRAS*, *NOTCH1*, *NPM1*, *PDGFRA*, *PTEN*, *PTPN11*, *RB1*, *RET*, *SMAD4*, *SMO*, *SRC*, *STK11*, and *VHL*.

HRAS Mutations Occurred Predominantly in EMCAs With Intact *PLAG1* and *HMGA2*

HRAS mutations were the most common genetic abnormality and were identified in 8 of 23 EMCAs (35%), including p.Q61R (n = 5), p.G13R (n = 1), p.Q61K (n = 1), and p.G13V (n = 1). All but 1 HRAS mutation occurred in EMCA with intact *PLAG1* and *HMGA2* (7/9 vs. 1/14, $P < 0.001$) (Fig. 8). One EMCA revealed concurrent HRAS p.Q61R and phosphoinositide-3-kinase catalytic alpha gene (PIK3CA) p.C420R mutations and intact *PLAG1* and *HMGA2*. PIK3CA exon 8 p.C420R mutation is located at the interface of the inner-SH2 of p38á and C2 domains and favors an active conformation of the protein, leading to overall increased phosphatidylinositol 3-kinase activity.[23,24]

Tumor Suppressor Alterations in High-grade EMCAs With Intact *PLAG1* and *HMGA2*

Three of the 7 (43%) high-grade EMCA cases examined by NGS harbored alterations in tumor suppressor genes, including TP53, *FBXW7*, and *SMARCB1*, and all of these tumors had intact *PLAG1* and *HMGA2*. No tumor suppressor alterations were identified in any examined conventional EMCA.

Case #22, a high-grade EMCA (Figs. 1A, 8) showed TP53 deletion and F-box and WD repeat domain containing 7 (*FBXW7*) p.R505L, c.1514G > T mutation. *FBXW7* is frequently mutated in head and neck squamous cell carcinomas, colorectal, and breast carcinomas and is believed to accelerate tumorigenesis, especially in the absence of functional TP53.[6,25,26]

Case #19, a high-grade EMCA (Fig. 1B), showed TP53 p.R273H, c.818G > A mutation in addition to HRAS p.Q61R.

Finally, case #20, a high-grade EMCA, showed *SMARCB1*/INI-1 deletion by NGS. This finding was corroborated by INI-1 immunohistochemistry and FISH (80% of tumor cells showed 22q monosomy and 20% of tumor cells showed homozygous *SMARCB1* deletion) (Fig. 9).

DISCUSSION

A variety of salivary gland carcinomas is believed to develop from PA. For instance, the majority of SDCs arise ex PA.[8,13,27] If *PLAG1* and *HMGA2* fusions are accepted as an objective marker of preexisting PA, the morphologic spectrum of carcinomas ex PA seems to be significantly narrower than previously thought. For instance, RNA sequencing and search for fusions did not identify *PLAG1* or *HMGA2* rearrangements in acinic cell carcinoma,[28] adenoid cystic carcinoma,[29] nor polymorphous adenocarcinoma.[30] Other salivary tumors rarely, if ever, show morphologic evidence of PA and are known to harbor distinct rearrangements that are most likely mutually exclusive with *PLAG1* and *HMGA2* alterations (eg, clear cell carcinoma,[31] mucoepidermoid carcinoma,[32] and mammary analog secretory carcinoma[33]). Indirectly and in the context of salivary tumors, these data suggest that the association of *PLAG1* and HMGA2 abnormalities with morphologic evidence of PA is quite specific. On the basis of combined morphologic and molecular evidence, in this series, the majority of EMCA (31/39, 80%) arose ex PA. The knowledge of *PLAG1* and *HMGA2* status may lead to wider acceptance of some of the subtler morphologic signs of preexisting PA, such as hypocellular hyalinized nodules, especially those without bland ducts.[13,34] The identification of preexisting PA varies with the extent of sampling. In this study, the need for abundant material and exclusion of samples with failed FISH or next-generation sequencing may have inadvertently lead to the bias toward more recent and more generously sampled cases. Anecdotally, it was shown that to identify preexisting PA one might have to examine up to a hundred tissue sections.

Previously, a cytogenetic study of 220 PAs characterized basic clinicopathologic features of adenomas with *PLAG1* and *HMGA2* rearrangements.[9] The prevalence of *PLAG1* abnormalities is similar in PAs and EMCAs (Table 2), suggesting that *PLAG1* alteration (without the knowledge of specific fusion partners) does not predispose a PA to malignant transformation to EMCA. However, *HMGA2* alterations seem to be more common in EMCAs than in PAs (Table 2).

The average age of patients with HMGA2-positive PA was 45.9 years,[9] while the average age of patients with HMGA2-positive EMCA in the current study was 69 years. This difference in patients' average age at initial presentation suggests that it may take about 24 years for an HMGA2-positive PA to progress to an EMCA.

It was previously reported that about 18% (11/61) of EMCAs show necrosis.[3] Here, the number of high-grade EMCA was 31% (12/39). This is perhaps partially explained by the referral of patients with more aggressive disease to tertiary medical centers ("pathology only" consultative cases were not included in this study). Of the cases previously reported by Fonseca and Soares,[2] 36% (8/22) of EMCAs showed necrosis, suggesting that the potential referral bias is similar between the contributing institutions.

One of the technical limitations of this project was the primary use of FISH to determine the status of *PLAG1* and *HMGA2*. *PLAG1* FISH is unlikely to identify intrachromosomal rearrangements, such as FGFR1-PLAG1, unless rearrangement is accompanied by *PLAG1* hyperploidy. This limitation was in part addressed in this study by testing all cases with *PLAG1* and *HMGA2* intact by FISH for *FGFR1-PLAG1* fusion by NGS.[22] Also, break-apart probes preclude identification of specific *PLAG1* or HMGA2 fusion partners. For instance, the list of potential *PLAG1* fusion partners includes leukemia inhibitory factor receptor, coiled-coil-helix-coiled-coil-helix domain containing 7, and CTNNB1 (beta-catenin).[10]

It seems that the factors involved in EMCA development depend on *PLAG1* and *HMGA2* status. We found little-to-no genetic changes in most EMCAs with HMGA2 or *PLAG1* alterations. The genetic events leading to transformation of PA into EMCA remain unknown and the NGS panel of 50 cancer-related genes used in this study apparently lacks the genes that may be involved in the development of *PLAG1*-driven or HMGA2-driven EMCAs.

Conversely, in EMCAs with intact *HMGA2* and *PLAG1*, HRAS mutations represent the most common alteration, followed by TP53, *FBXW7*, and *SMARCB1* in high-grade EMCAs. Variant morphologies, such as oncocytic and apocrine EMCA, were only represented singly in this study and it is unclear whether these have a distinct molecular profile.

A number of *PLAG1*-intact or *HMGA2*-intact conventional EMCA are driven by HRAS, rarely accompanied by PIK3CA mutations. HRAS mutations have been implicated in salivary tumorigenesis as early as the 1990s: transgenic mice expressing an HRAS p.G12V mutation developed “adenosquamous” carcinomas of submandibular glands.[35] Since then a variety of common tumor types including carcinoma ex PA and adenocarcinoma, not otherwise specified, have been reported to have HRAS mutations or protein p21 overexpression.[15,36] PIK3CA is one of the better known effectors of HRAS and HRAS/PIK3CA cooperation is crucial to HRAS-induced skin cancer formation.[37,38] PIK3CA encodes the p110á catalytic subunit of the class IA phosphatidylinositol 3-kinase. PIK3CA exon 8 p.C420R mutation disrupts the interaction between the inner-SH2 of p38á and C2 domains and increases the lipid kinase activity.[23,24]

One of 23 tested EMCAs showed *SMARCB1* loss, indicating that EMCA may join the growing list of tumors with *SMARCB1* loss.[39] This tumor was of high histologic grade and demonstrated overgrowth of the myoepithelial component; interestingly, *SMARCB1*/INI-1 immunohisto-chemistry revealed loss of nuclear *SMARCB1*/INI-1 staining predominantly in myoepithelial, but not ductal cells (Fig. 9), suggesting that *SMARCB1* loss may be a driving molecular event in the high-grade transformation of the myoepithelial component.

Practically, the complexity of the morphologic and genetic findings in EMCA confounds correlation with clinicopathologic parameters. Potential therapeutic options for clinically aggressive EMCAs include targeting of mammalian target of rapamycin or mitogen-activated protein kinase/extracellular signal-regulated kinases inhibitors for cases with

HRAS+/−PIK3CA mutations[40] or indirect RAS targeting through inhibition of farnesyl transferase (one of the EMCAs in this study was tested clinically with this option in mind).[40]

In summary, morphologically and molecularly (ie, *PLAG1* and *HMGA2*) up to 80% of EMCA arise from PA and in some clinical settings the proportion of high-grade EMCA can be as high as 30%. The genetic profile of *EMCA* varies with the *PLAG1* and *HMGA2* status. *PLAG1* and *HMGA2* intact cases tend to have HRAS mutations that are evenly distributed between conventional and high-grade EMCAs. High-grade EMCAs with intact *PLAG1* and *HMGA2* showed TP53, SMARCB1, and *FBXW7* alterations.

ACKNOWLEDGMENTS

The authors wish to thank members of the Division of the Molecular and Genomic Pathology and Developmental Laboratory of the Department of Pathology for excellent technical support.

REFERENCES

1. Corio RL, Sciubba JJ, Brannon RB, et al. Epithelial-myoepithelial carcinoma of intercalated duct origin. A clinicopathologic and ultrastructural assessment of sixteen cases. Oral Surg Oral Med Oral Pathol. 1982;53:280–287. [PubMed: 6950345]
2. Fonseca I, Soares J. Epithelial-myoepithelial carcinoma of the salivary glands. A study of 22 cases. Virchows Arch A Pathol Anat Histopathol. 1993;422:389–396. [PubMed: 8322454]
3. Seethala RR, Barnes EL, Hunt JL. Epithelial-myoepithelial carcinoma: a review of the clinicopathologic spectrum and immunophenotypic characteristics in 61 tumors of the salivary glands and upper aerodigestive tract. Am J Surg Pathol. 2007;31:44–57. [PubMed: 17197918]
4. Donath K, Seifert G, Schmitz R. [Diagnosis and ultrastructure of the tubular carcinoma of salivary gland ducts. Epithelial-myoepithelial carcinoma of the intercalated ducts] Virchows Arch A Pathol Pathol Anat. 1972;356:16–31. [PubMed: 4340536]
5. Alos L, Carrillo R, Ramos J, et al. High-grade carcinoma component in epithelial-myoepithelial carcinoma of salivary glands clinicopathological, immunohistochemical and flow-cytometric study of three cases. Virchows Arch. 1999;434:291–299. [PubMed: 10335939]
6. Daa T, Kashima K, Gamachi A, et al. Epithelial-myoepithelial carcinoma harboring p53 mutation. APMIS. 2001;109:316–320. [PubMed: 11469504]
7. Roy P, Bullock MJ, Perez-Ordonez B, et al. Epithelial-myoepithelial carcinoma with high grade transformation. Am J Surg Pathol. 2010;34:1258–1265. [PubMed: 20679885]
8. Williams L, Thompson LD, Seethala RR, et al. Salivary duct carcinoma: the predominance of apocrine morphology, prevalence of histologic variants, and androgen receptor expression. Am J Surg Pathol. 2015;39:705–713. [PubMed: 25871467]
9. Bullerdiek J, Wobst G, Meyer-Bolte K, et al. Cytogenetic subtyping of 220 salivary gland pleomorphic adenomas: correlation to occurrence, histological subtype, and in vitro cellular behavior. Cancer Genet Cytogenet. 1993;65:27–31. [PubMed: 8381711]
10. Stenman G. Fusion oncogenes in salivary gland tumors: molecular and clinical consequences. Head Neck Pathol. 2013;7 (Suppl 1): S12–S19. [PubMed: 23821214]
11. Katabi N, Ghossein R, Ho A, et al. Consistent PLAG1 and HMGA2 abnormalities distinguish carcinoma ex-pleomorphic adenoma from its de novo counterparts. Hum Pathol. 2015;46:26–33. [PubMed: 25439740]
12. Bahrami A, Dalton JD, Shivakumar B, et al. PLAG1 alteration in carcinoma ex pleomorphic adenoma: immunohistochemical and fluorescence in situ hybridization studies of 22 cases. Head Neck Pathol. 2012;6:328–335. [PubMed: 22485045]
13. Chiosea SI, Thompson LD, Weinreb I, et al. Subsets of salivary duct carcinoma defined by morphologic evidence of pleomorphic adenoma, PLAG1 or HMGA2 rearrangements, and common genetic alterations. Cancer. 2016;122:3136–3144. [PubMed: 27379604]

14. Chetty R. Intercalated duct hyperplasia: possible relationship to epithelial-myoepithelial carcinoma and hybrid tumours of salivary gland. Histopathology. 2000;37:260–263. [PubMed: 10971702]
15. Cros J, Sbidian E, Hans S, et al. Expression and mutational status of treatment-relevant targets and key oncogenes in 123 malignant salivary gland tumours. Ann Oncol. 2013;24:2624–2629. [PubMed: 23933559]
16. Chiosea SI, Miller M, Seethala RR. HRAS mutations in epithelialmyoepithelial carcinoma. Head Neck Pathol. 2014;8:146–150. [PubMed: 24277618]
17. Seethala RR, Richmond JA, Hoschar AP, et al. New variants of epithelial-myoepithelial carcinoma: oncocytic-sebaceous and apocrine. Arch Pathol Lab Med. 2009;133:950–959. [PubMed: 19492889]
18. Edge DRBSB, Compton CC, Fritz AG, et al. AJCC Cancer Staging Handbook: From the AJCC Cancer Staging Manual. New York: Springer; 2009.
19. Roy S, Durso MB, Wald A, et al. SeqReporter: automating next-generation sequencing result interpretation and reporting workflow in a clinical laboratory. J Mol Diagn. 2014;16:11–22. [PubMed: 24220144]
20. Liu X, Jian X, Boerwinkle E. dbNSFP: a lightweight database of human nonsynonymous SNPs and their functional predictions. Hum Mutat. 2011;32:894–899. [PubMed: 21520341]
21. Grasso C, Butler T, Rhodes K, et al. Assessing copy number alterations in targeted, amplicon-based next-generation sequencing data. J Mol Diagn. 2015;17:53–63. [PubMed: 25468433]
22. Beadling C, Wald AI, Warrick A, et al. A Multiplexed Amplicon Approach for Detecting Gene Fusions by Next-Generation Sequencing. J Mol Diagn. 2016;18:165–175. [PubMed: 26747586]
23. Burke JE, Perisic O, Masson GR, et al. Oncogenic mutations mimic and enhance dynamic events in the natural activation of phosphoinositide 3-kinase p110alpha (PIK3CA). Proc Natl Acad Sci U S A. 2012;109:15259–15264. [PubMed: 22949682]
24. Gymnopoulos M, Elsliger MA, Vogt PK. Rare cancer-specific mutations in PIK3CA show gain of function. Proc Natl Acad Sci U S A. 2007;104:5569–5574. [PubMed: 17376864]
25. Xu W, Taranets L, Popov N. Regulating Fbw7 on the road to cancer. Semin Cancer Biol. 2016;36:62–70. [PubMed: 26459133]
26. Agrawal N, Frederick MJ, Pickering CR, et al. Exome sequencing of head and neck squamous cell carcinoma reveals inactivating mutations in NOTCH1. Science. 2011;333:1154–1157. [PubMed: 21798897]
27. Griffith CC, Thompson LD, Assaad A, et al. Salivary duct carcinoma and the concept of early carcinoma ex pleomorphic adenoma. Histopathology. 2014;65:854–860. [PubMed: 24804831]
28. Barasch N, Gong X, Kwei KA, et al. Recurrent rearrangements of the Myb/SANT-like DNA-binding domain containing 3 gene (MSANTD3) in salivary gland acinic cell carcinoma. PLoS One. 2017;12:e0171265. [PubMed: 28212443]
29. Rettig EM, Talbot CC Jr, Sausen M, et al. Whole-Genome Sequencing of Salivary Gland Adenoid Cystic Carcinoma. Cancer Prev Res (Phila). 2016;9:265–274. [PubMed: 26862087]
30. Weinreb I, Zhang L, Tirunagari LM, et al. Novel PRKD gene rearrangements and variant fusions in cribriform adenocarcinoma of salivary gland origin. Genes Chromosomes Cancer. 2014;53:845–856. [PubMed: 24942367]
31. Antonescu CR, Katabi N, Zhang L, et al. EWSR1-ATF1 fusion is a novel and consistent finding in hyalinizing clear-cell carcinoma of salivary gland. Genes Chromosomes Cancer. 2011;50:559–570. [PubMed: 21484932]
32. Tonon G, Modi S, Wu L, et al. t(11;19)(q21;p13) translocation in mucoepidermoid carcinoma creates a novel fusion product that disrupts a Notch signaling pathway. Nat Genet. 2003;33:208–213. [PubMed: 12539049]
33. Skalova A, Vanecek T, Sima R, et al. Mammary analogue secretory carcinoma of salivary glands, containing the ETV6-NTRK3 fusion gene: a hitherto undescribed salivary gland tumor entity. Am J Surg Pathol. 2010;34:599–608. [PubMed: 20410810]
34. Bahrami A, Perez-Ordonez B, Dalton JD, et al. An analysis of PLAG1 and HMGA2 rearrangements in salivary duct carcinoma and examination of the role of precursor lesions. Histopathology. 2013;63:250–262. [PubMed: 23738717]

35. Nielsen LL, Discafani CM, Gurnani M, et al. Histopathology of salivary and mammary gland tumors in transgenic mice expressing a human Ha-ras oncogene. Cancer Res. 1991;51:3762–3767. [PubMed: 2065330]

36. Augello C, Gregorio V, Bazan V, et al. TP53 and p16INK4A, but not H-KI-Ras, are involved in tumorigenesis and progression of pleomorphic adenomas. J Cell Physiol. 2006;207:654–659. [PubMed: 16447252]

37. Gupta S, Ramjaun AR, Haiko P, et al. Binding of ras to phosphoinositide 3-kinase p110alpha is required for ras-driven tumorigenesis in mice. Cell. 2007;129:957–968. [PubMed: 17540175]

38. Castellano E, Downward J. RAS Interaction with PI3K: More Than Just Another Effector Pathway. Genes Cancer. 2011;2:261–274. [PubMed: 21779497]

39. Agaimy A. The expanding family of SMARCB1(INI1)-deficient neoplasia: implications of phenotypic, biological, and molecular heterogeneity. Adv Anat Pathol. 2014;21:394–410. [PubMed: 25299309]

40. Brock EJ, Ji K, Reiners JJ, et al. How to Target Activated Ras Proteins: Direct Inhibition vs. Induced Mislocalization. Mini Rev Med Chem. 2016;16:358–369. [PubMed: 26423696]

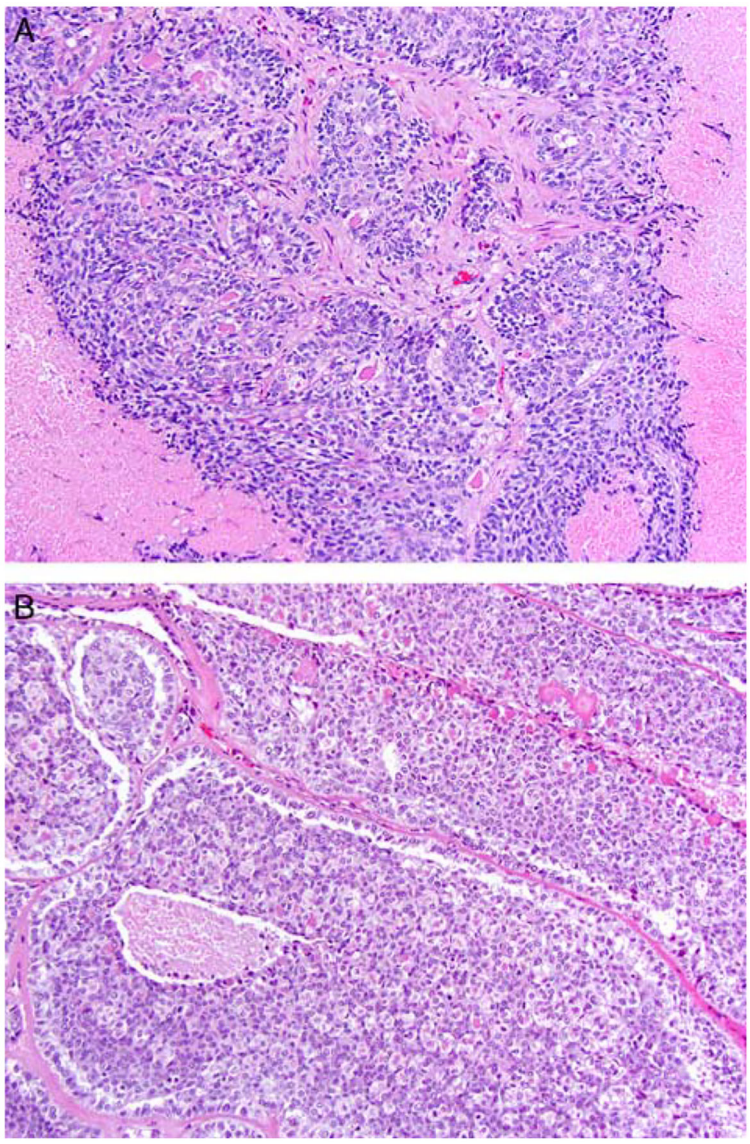

FIGURE 1.

High-grade EMCA. A, Islands of viable EMCA are surrounded by coagulative necrosis. Case #22, see also Figure 8. Abluminal myoepithelial cells with clear cytoplasm are slightly more predominant over occasional small ducts filled with eosinophilic secretions. Hematoxylin and eosin (H&E) stain. B, Myoepithelial cells outlining the lobules of predominant small ducts. The comedo-type necrosis is in the left lower quadrant of the image. Note retraction/split artifact between the single layer of myoepithelial cells arranged along the thin septae and ductal cells. Case #19, see also Figure 8 (H&E stain).

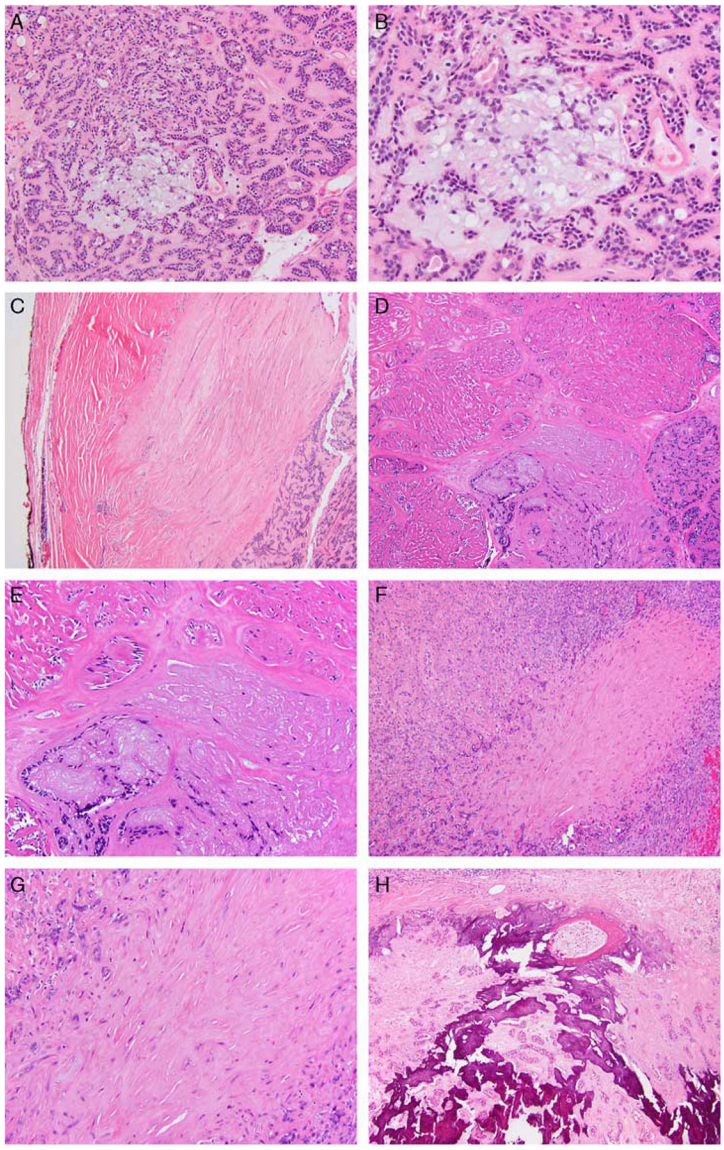

FIGURE 2.

Morphologic evidence of PA. A–C, Areas of residual PA in a case of EMCA with HMGA2 rearrangement, case #1 in Figure 8. (Note: areas diagnostic of invasive EMCA are not shown.) A, One of several foci of chondromyxoid stroma, H&E stain. B, The same focus of chondromyxoid stroma as shown in (A), at higher magnification, H&E. C, Capsule/periphery of the preexisting PA represented by condensed hypocellular hyalinized stroma, H&E. D and E, EMCA ex PA, case #2 in Figure 8. D, Lobules of hypocellular hyalinized and myxoid stroma, H&E. F and G, One of several rounded hyalinized scars in an EMCA with *PLAG1* rearrangement, case #9 in Figure 8 (H&Es: F, G). H, Heavy calcification and osseous metaplasia in a PA with *PLAG1* rearrangement, case #13 in Figure 8, H&E.

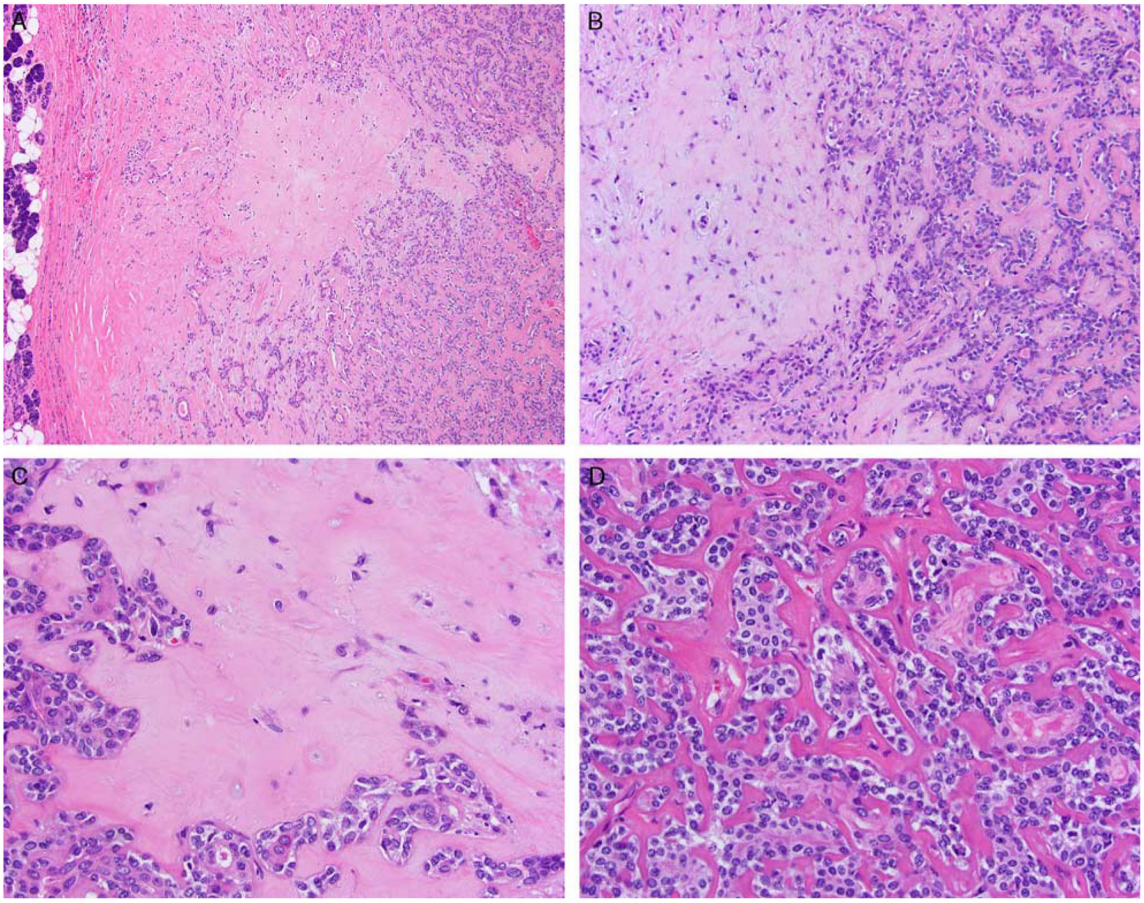

FIGURE 3.

Morphologic evidence of preexisting PA in an EMCA with *HMGA2* rearrangement, case #7 in Figure 8. A, Note the rim of normal parotid tissue, left. In the center of the image there is a focus of hyalinized hypocellular stroma, H&E. B, Another lobule of chondromyxoid stroma, H&E. C, Lobule of chondroid stroma, H&E. D, EMCA component with clear myoepithelial cells and eosinophilic ductal cells. The cellular component is sharply demarcated from hyalinized stroma, H&E.

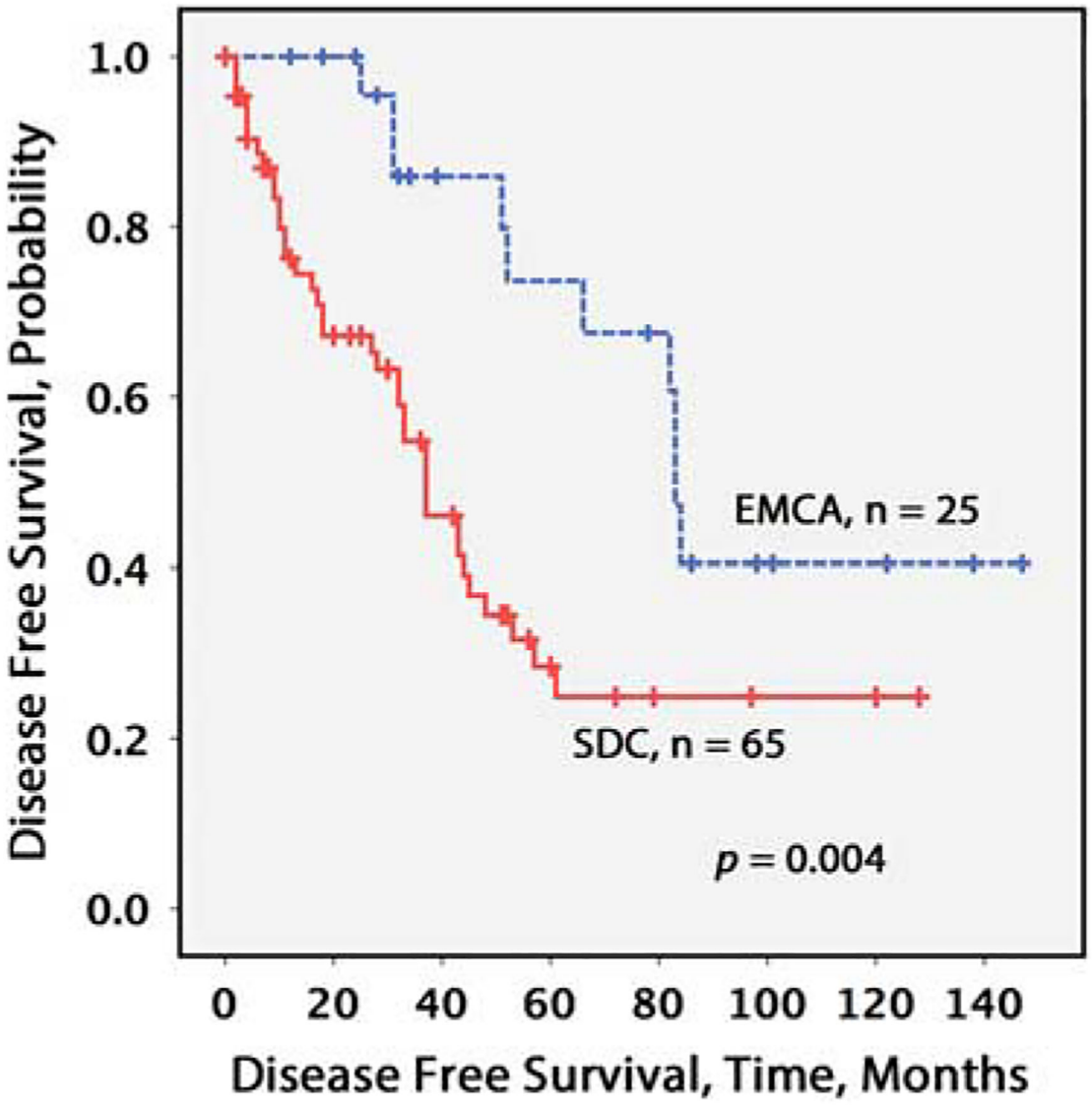

FIGURE 4.

Kaplan-Meier plot, estimated DFS of patients with EMCA, compared with patients with SDC (from Chiosea et al).[13]

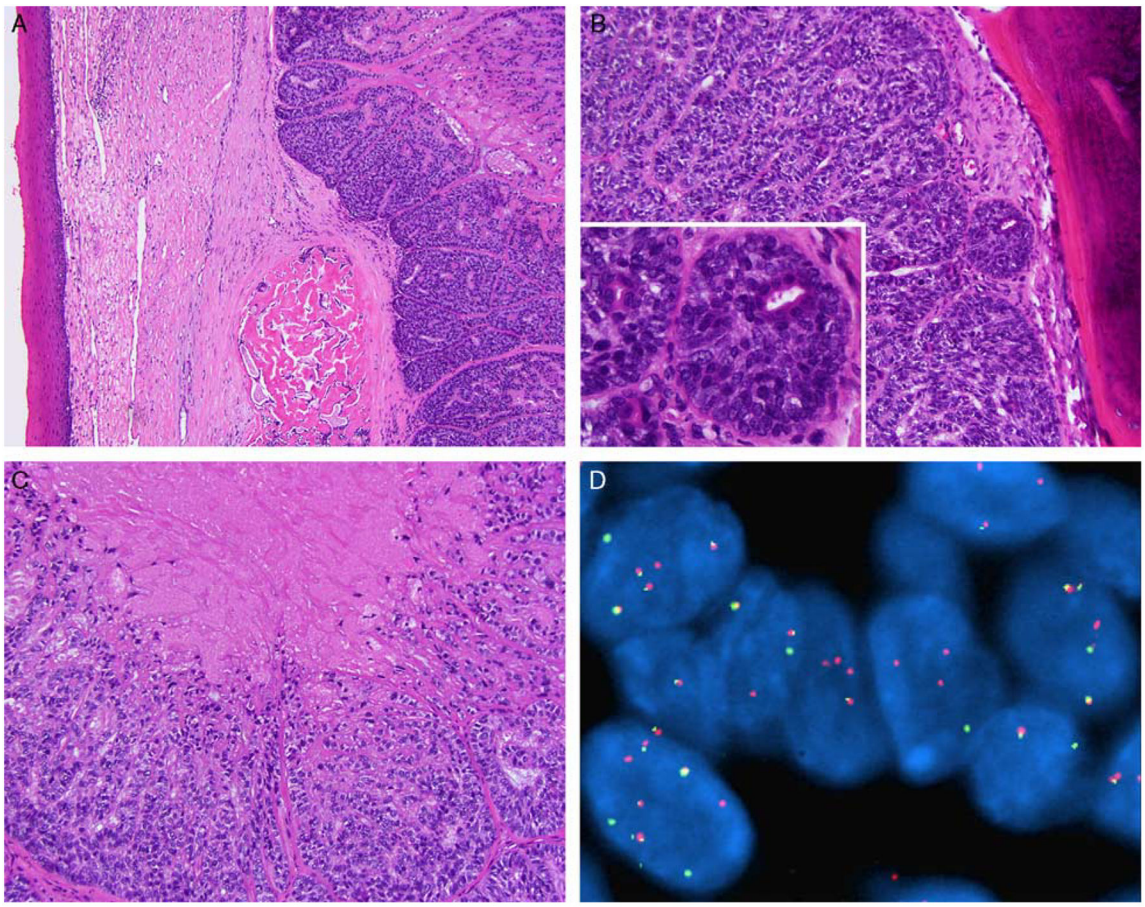

FIGURE 5.

High-grade EMCA with morphologic evidence of PA, necrosis, and HMGA2 rearrangement and hyperploidy. Case #2, see also Figure 8. A, Uninvolved squamous mucosa of the palate overlying an EMCA. Note hyalinized hypocellular stroma of preexisting PA in the lower mid part of the image, H&E. B, EMCA extending to the maxillary bone. Rare ducts are surrounded by predominant myoepithelial cells, H&E and inset. C, Necrosis, H&E. D, *HMGA2* break-apart FISH. Intact *HMGA2* signal is yellow, while rearrangement is indicated by red and green signals. DAPI (4′,6-diamidino-2-phenylindole) outlines nuclei.

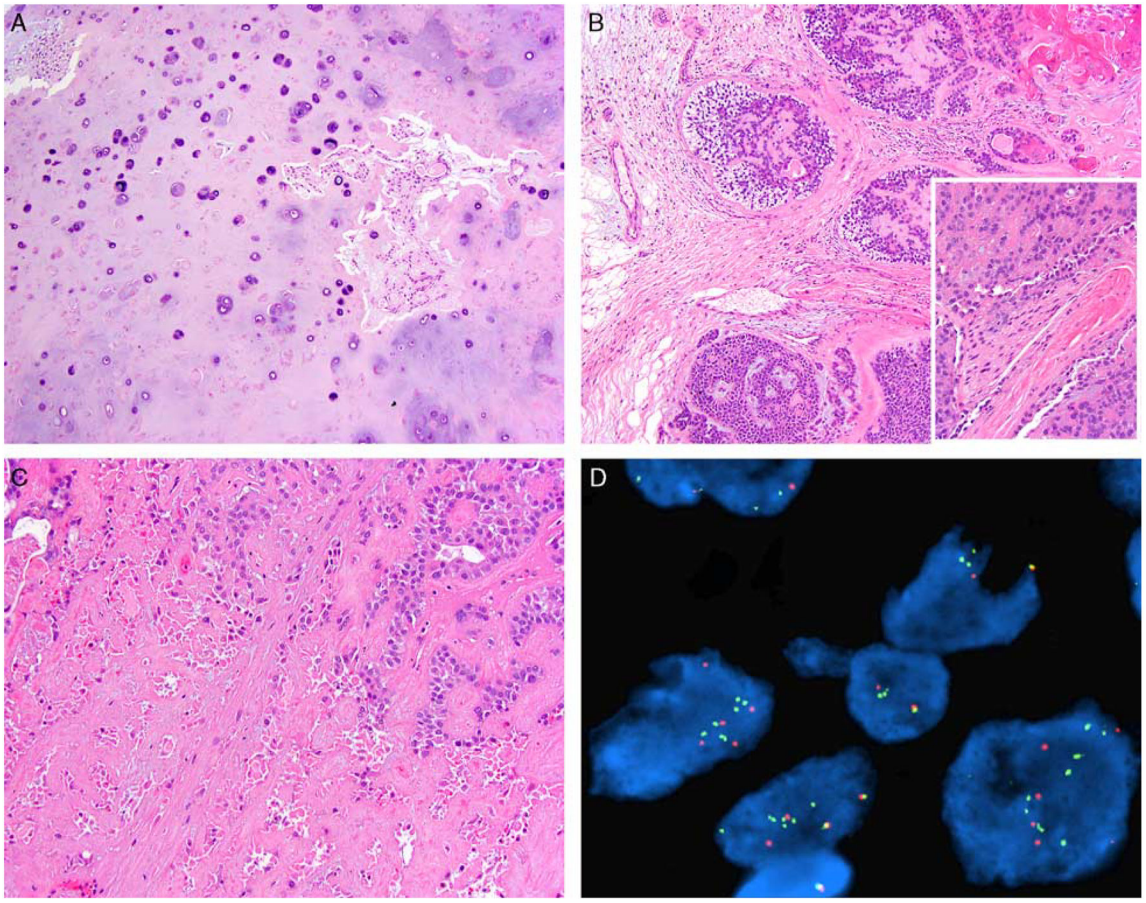

FIGURE 6.

High-grade EMCA with morphologic evidence of PA, necrosis, and *PLAG1* rearrangement and hyperploidy; case #13 in Figure 8. A, Preexisting PA was represented by lobules of chondromyxoid stroma with embedded rare bland ducts and myoepithelial cells, H&E. B, EMCA was infiltrative, with perineural invasion (inset, lower right), H&E. C, Necrosis, H&E. D, *PLAG1* break-apart FISH. Intact *PLAG1* signal is yellow, while rearrangement is indicated by distinct red and green signals. DAPI (4′,6-diamidino-2-phenylindole) outlines nuclei.

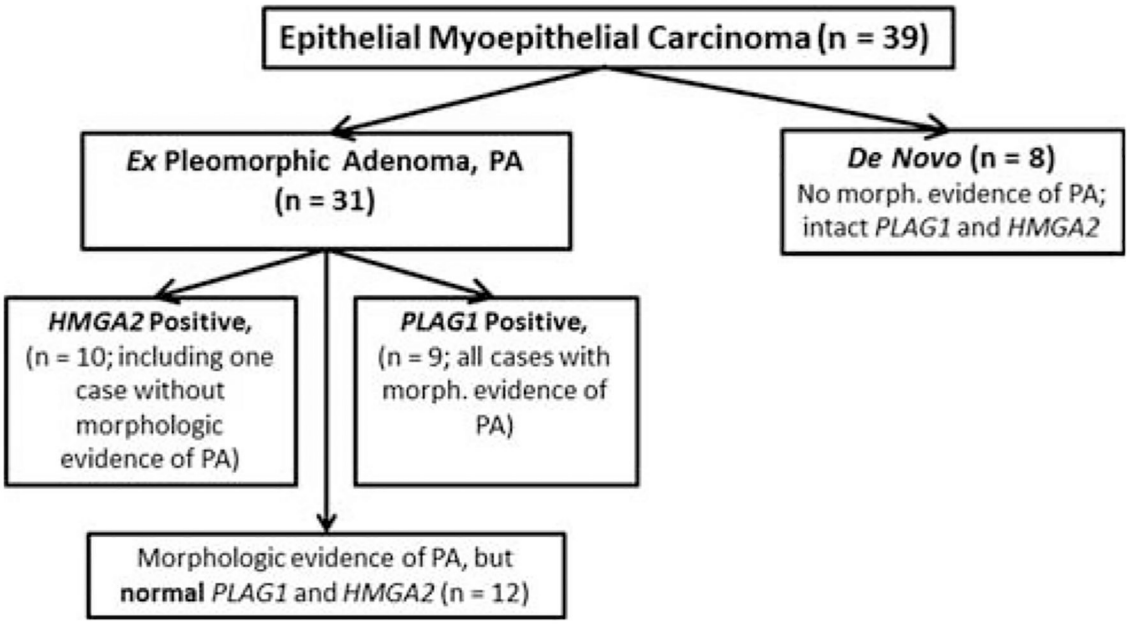

FIGURE 7.

Subsets of EMCA: relationship between the morphologic evidence of PA and *PLAG1* or *HMGA2* status.

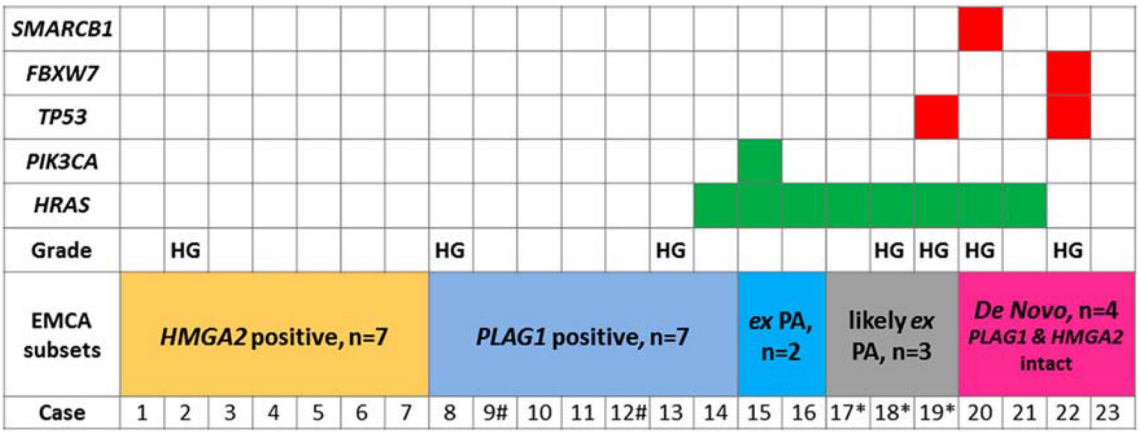

FIGURE 8.

The relationship between the subsets of EMCA and histologic grade, mutations, and copy number variation in 50 cancer-related genes. Only genes with mutations or copy number alterations are shown (first column). Mutations (TP53, *FBXW7*) and deletions (SMARCB1) in tumor suppressor genes are highlighted in red. Mutations in oncogenes are highlighted in green. *Cases for which only recurrent tumor was rereviewed for this study (initial resections were diagnosed as PA). #Cases with *FGFR1-PLAG1* fusion identified by next-generation sequencing. HG indicates high grade.

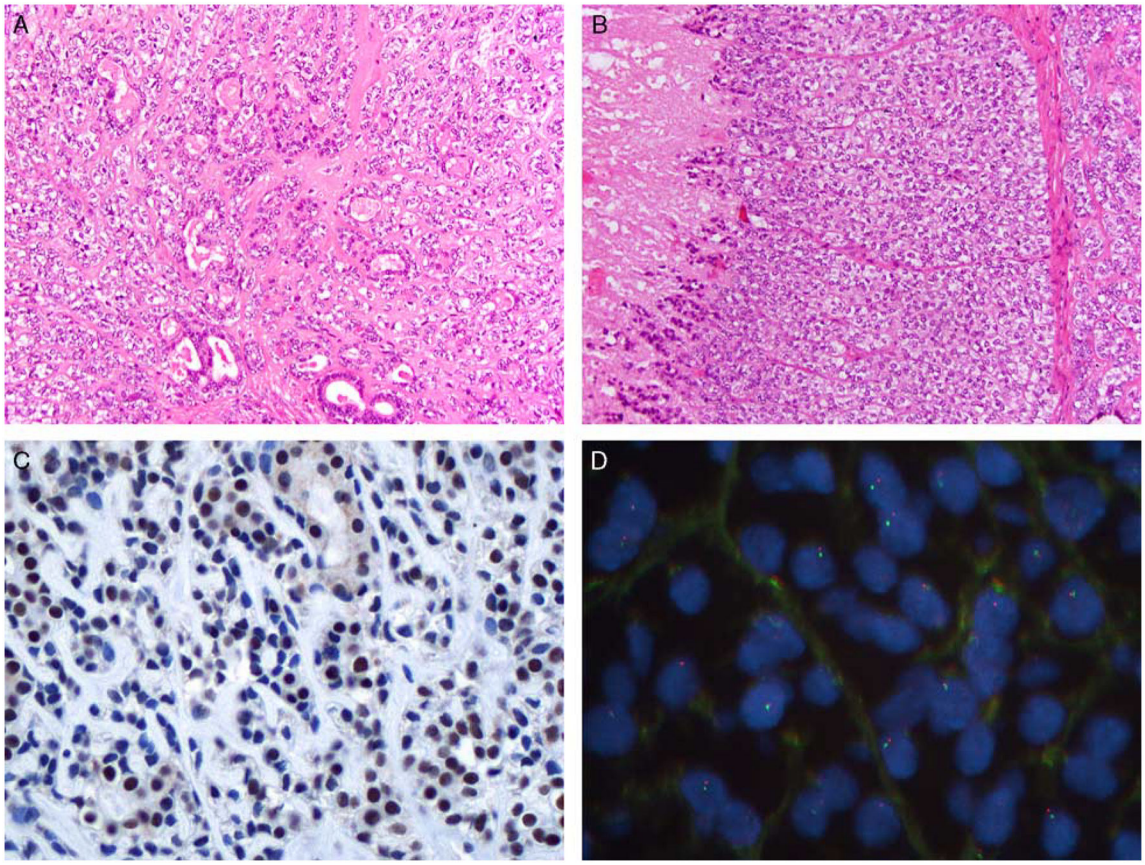

FIGURE 9.

High-grade EMCA de novo with *SMARCB1*/INI-1 loss; case #20 in Figure 8. A, Areas with ducts and clear myoepithelial cells, H&E. B, Areas with solid growth of clear myoepithelial cells and necrosis, H&E. C, SMARCB1/INI-1 loss predominantly in myoepithelial cells, immunohistochemistry. D, *SMARCB1* FISH. DAPI (4′,6-diamidino-2-phenylindole) outlines nuclei.

TABLE 1.

Clinicopathologic Features of Patients With EMCA

Sex, Female (n/N [%])	25/39 (64)
Age (mean [range]) (y)	66 (19–87)
Anatomic site (n [%])	
Parotid gland	22 (57)
Palate	8 (20)
Submandibular gland	5 (13)
Minor salivary glands (eg, nasal cavity)	4 (10)
pT (n [%])	
x	4 (10)
1	6 (15)
2	16 (41)
3	10 (26)
4	3 (8)
pN (n [%])	
x	19 (49)
0	19 (49)
1	1 (2)
M (n [%])	
cM0	38 (98)
pM1	1 (2)

TABLE 2.

Prevalence of *PLAG1* or *HMGA2* Alteration and Average Age of Patients With PA (Literature Review) and EMCA

	Patients' Age (Average [Range, for Patients in the Current Study]) (y)		Prevalence of Alterations (n/N [%])	
	PA*	EMCA	PA*	EMCA
Patients with tumors carrying *PLAG1* alteration	39	65 (47–83)	56/220 (25.5)	9/39 (23)
Patients with tumors carrying *HMGA2* alteration	45.9	69 (46–85)	29/220 (13.2)	10/39 (26)

* The data on patients with PA are from Bullerdiek et al.[9]